*Quantum Electronics* **44** (12) 1112–1118 (2014) 

*METAMATERIALS*

PACS numbers: 81.05.Xj; 78.67.Pt; 73.20.Mf
DOI: 10.1070/QE2014v044n12ABEH015559

# Focusing of dipole radiation by a negative index chiral layer. 2. A thin layer as compared with the wavelength

D.V. Guzatov, V.V. Klimov

***Abstract.*** **Using the quasi-static approximation we have found exact analytical solutions to the problem of the field of a point electromagnetic source in the presence of a layer of a bi-isotropic (chiral) metamaterial. At some parameters of the problem, the resulting solution can be represented as a set of several point sources (electric and magnetic), which are images of the original source. If the original source is located near the layer, these images become real sources of the field. This paradoxical solution is then generalised to the case taking into account the retardation effects, which allows one to physically interpret the obtained solutions as a set of sources and 'sinks' of circularly polarised waves.**

***Keywords:*** *chiral metamaterial, negative refractive index, quasi-static approximation, plasmons.*

## 1. Introduction

Calculation of emission of a point source near a layer of a material of finite thickness is a classical electrodynamics problem, the history of which begins with the work of Sommerfeld published in the early 20th century [1]. Despite the simplicity of the geometry, this problem is very complex and has been widely discussed (see, for example, [2]).

The situation has become even more interesting after Veselago [3] and Pendry [4] published their works, in which they assumed that if a layer is made of a double negative (DNG) metamaterial, which simultaneously has negative permittivity and permeability, it can become an interesting focusing device – a perfect lens (Fig. 1). Further analysis showed, however, that the geometry presented in Fig. 1 is realised only for relatively thick layers and not too small losses in them. In the case of thin layers and small losses in the layer, surface plasmons are excited and perfect focusing does not arise, whereas instead of focus there is a saddle point (see, for example, [5]). An alternative to using a negative index layer was considered in [6–8], in which instead of a single source the authors proposed to employ two symmetrical sources and a 'sink'. (This approach has recently again aroused interest [9].) Under such a formulation of the problem, surface plasmons are not excited and we deal with real perfect focusing. Using the analytical solutions [6–8] the authors of papers [10, 11] managed to produce a new type of optical nanodevices, i.e., coherent nanoabsorbers.

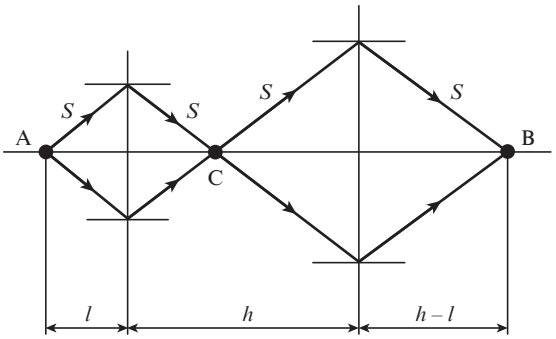


**Figure 1.** Geometry of focusing of light by a negative index layer [3]. Emission from a source located at point A at a distance $l$ from the layer of thickness $h$ is focused behind the layer and inside it at points B and C, respectively. Arrows indicate the direction of the energy flow, $S$.

Further development of the applications of this geometry is to investigate a layer made of a negative index bi-isotropic (chiral) metamaterial. The prospect of such a formulation of the problem stems from the fact that chirality is closely associated with a negative refractive index [12] and, therefore, we can expect to see many interesting effects, primarily related to perfect focusing of circularly polarised waves and to fabrication of coherent nanoabsorbers of these waves by analogy with simple coherent nanoabsorbers [8, 10].

The first results in this direction were obtained in our previous work [13], where we studied the possibility of focusing radiation from a point source by a chiral DNG layer whose thickness is much greater than the radiation wavelength. We showed that such a layer can be treated as a lens that focuses right- and left-hand polarised waves in a different way and has a greater flexibility in the manipulation of the focal length as compared with a conventional Veselago lens [3]. However, in spite of a negative refractive index the focusing system considered in [13] did not exhibit perfect focusing properties, i.e., the size of the focal spot turned out to be diffraction-limited. This was due to the fact that the thickness of the focusing layer is much greater than the radiation wavelength and absorption in the layer is sufficiently high. In this paper (which is a direct continuation of [13]), we consider the opposite case, when the layer thickness is much smaller than the wavelength, absorption is small or absent and the source can be brought closer to the layer to a distance that is less than the thickness of the latter. This case is interesting from two points

**D.V. Guzatov** Yanka Kupala State University of Grodno, ul. Ozheshko 22, 230023 Grodno, Belarus; e-mail: dm_guzatov@mail.ru;
**V.V. Klimov** P.N. Lebedev Physics Institute, Russian Academy of Sciences, Leninsky prosp. 53, 119991 Moscow, Russia; National Research Nuclear University MEPhI, Kashirskoe shosse 31, 115409 Moscow, Russia; e-mail: vklim@sci.lebedev.ru

Received 16 May 2014; revision received 19 September 2014
*Kvantovaya Elektronika* **44** (12) 1112–1118 (2014)
Translated by I.A. Ulitkin

of view. On the one hand, such layers (nanolayers) may be integrated into advanced optical nanodevices, while on the other, the physics of optical phenomena in them is significantly different than that in thick layers as compared with the wavelength and in some sense is paradoxical (see below).

The general solution to the problem of radiation from a point source near a chiral layer with arbitrary parameters was found in [13], but it is very cumbersome and difficult for the analysis. Therefore, in this paper our study is first performed in the framework of the quasi-static approximation when we can neglect the retardation effects. In the case of a source located with respect to the nanolayer at a distance less than the wavelength, this approximation is quite justified, and the analytical solution obtained allows a deeper understanding of the physics of the proceeding phenomena.

This paper is organised as follows. In Section 2 we obtain a general quasi-static solution to the problem of the total field of electric and magnetic dipoles (chiral dipole) near a chiral layer. In Section 3 we consider the case of a lossless chiral DNG layer (i.e. the imaginary parts of the permittivity and permeability in the layer are exactly equal to zero) and show that the solution radically changes as compared with a low-loss layer. In Section 4 the paradoxical solution found in Section 3 is generalised with the retardation effects taken into account. This generalisation allows us to understand the physical meaning of the solution: A negative index chiral layer is not a perfect lens for circularly polarised waves (in the sense of the Pendry–Veselago perfect lens), but allows one to focus radiation of two symmetrically arranged circularly polarised point sources in an arbitrarily small region (sink).

## 2. A point source near a low-loss chiral layer (quasi-static approximation)

Consider a source with electric and magnetic dipole moments $\boldsymbol{d}_0$ and $\boldsymbol{m}_0$, respectively (Fig. 2), located at point $z_0$ ($z_0 > 0$) on the $z$ axis of the Cartesian coordinate system in a semi-infinite medium 1 (vacuum, $\varepsilon_1 = \mu_1 = 1$). The chiral metamaterial layer 2, which is thin as compared with the wavelength and has thickness $h$, is located in the region $-h < z < 0$. The permittivity and permeability of the chiral material are denoted by $\varepsilon_2$ and $\mu_2$, respectively, and the chirality parameter – by $\chi_2$. As in our previous work [13], we consider a layer of a chiral material, described by the Drude–Born–Fedorov constitutive equations [14–16]

$$k_0\boldsymbol{D}_2 = \varepsilon_2(k_0\boldsymbol{E}_2 + \chi_2 \mathrm{rot}\boldsymbol{E}_2),\ k_0\boldsymbol{B}_2 = \mu_2(k_0\boldsymbol{H}_2 + \chi_2 \mathrm{rot}\boldsymbol{H}_2), \quad (1)$$

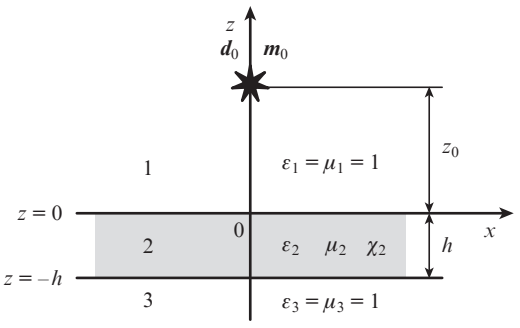


**Figure 2.** Geometry of the problem for a dipole source located near a thin chiral layer.

where $\boldsymbol{D}_2$, $\boldsymbol{B}_2$ are the inductions and $\boldsymbol{E}_2$, $\boldsymbol{H}_2$ are the electric and magnetic field strengths, respectively; and $k_0 = \omega/c$ is the wavenumber in vacuum. The factor $\exp(-i\omega t)$, which determines the time dependence of the fields, is omitted. Behind the chiral layer there is a semi-infinite medium 3 (vacuum, $\varepsilon_3 = \mu_3 = 1$). Note that the case of media 1 and 3 with different values of permittivity and permeability can be treated similarly.

To describe the fields near a thin ($k_0 h \ll 1$) chiral layer, we will use the quasi-static approximation. The expressions for the electric and magnetic fields of the source can be written using the potentials as follows ($z > 0$):

$$\begin{aligned} \boldsymbol{E}_0 &= -\nabla\phi_0^E, \quad \phi_0^E = -(\boldsymbol{d}_0\nabla)\frac{1}{|\boldsymbol{r}-\boldsymbol{r}_0|}, \\ \boldsymbol{H}_0 &= -\nabla\phi_0^H, \quad \phi_0^H = -(\boldsymbol{m}_0\nabla)\frac{1}{|\boldsymbol{r}-\boldsymbol{r}_0|}, \end{aligned} \quad (2)$$

where $\nabla$ is the gradient operator; and $\boldsymbol{r}$ and $\boldsymbol{r}_0$ are the radius vectors of the observation point and source position, respectively.

For the convenience of further calculations, we write expressions for the potentials $\phi_0^E$ and $\phi_0^H$ in integral form (see, for example, [17]):

$$\begin{Bmatrix}\phi_0^E\\ \phi_0^H\end{Bmatrix} = \left(\begin{Bmatrix}d_{0x}\\ m_{0x}\end{Bmatrix}\cos\varphi + \begin{Bmatrix}d_{0y}\\ m_{0y}\end{Bmatrix}\sin\varphi\right)\int_0^\infty \mathrm{d}q q J_1(q\rho)$$
$$\times\exp(-q|z-z_0|) \pm \begin{Bmatrix}d_{0z}\\ m_{0z}\end{Bmatrix}\int_0^\infty \mathrm{d}q q J_0(q\rho)\exp(-q|z-z_0|), \quad (3)$$

where $0 \leqslant \rho < \infty$ and $0 \leqslant \varphi < 2\pi$ are the polar coordinates; $J_n(q\rho)$ is the Bessel function [18]; and the 'plus' sign in front of the last term in (3) corresponds to the case $z > z_0$ and the 'minus' sign – to the case $z < z_0$.

We also write the expressions for the scattered electric and magnetic fields using the potentials. For field strengths $\boldsymbol{E}_1$, $\boldsymbol{H}_1$ in a half-space 1 ($z > 0$), we have

$$\boldsymbol{E}_1 = -\nabla\phi_1^E,\ \boldsymbol{H}_1 = -\nabla\phi_1^H,\ \begin{Bmatrix}\phi_1^E\\ \phi_1^H\end{Bmatrix} = \sum_{n=0}^{1}\int_0^\infty \mathrm{d}q q J_n(q\rho)$$
$$\times\left[\begin{Bmatrix}A_{nq1}^E\\ A_{nq1}^H\end{Bmatrix}\cos(n\varphi) + \begin{Bmatrix}B_{nq1}^E\\ B_{nq1}^H\end{Bmatrix}\sin(n\varphi)\right]\exp(-qz). \quad (4)$$

For the scattered field strengths $\boldsymbol{E}_2$, $\boldsymbol{H}_2$ in the chiral layer ($-h < z < 0$) we can write the expressions

$$\boldsymbol{E}_2 = -\nabla\phi_2^E,\ \boldsymbol{H}_2 = -\nabla\phi_2^H,\ \begin{Bmatrix}\phi_2^E\\ \phi_2^H\end{Bmatrix} = \sum_{n=0}^{1}\int_0^\infty \mathrm{d}q q J_n(q\rho)$$
$$\times\left\{\left[\begin{Bmatrix}A_{nq2}^E\\ A_{nq2}^H\end{Bmatrix}\cos(n\varphi) + \begin{Bmatrix}B_{nq2}^E\\ B_{nq2}^H\end{Bmatrix}\sin(n\varphi)\right]\exp(-qz)\right. \quad (5)$$
$$\left.+\left[\begin{Bmatrix}C_{nq2}^E\\ C_{nq2}^H\end{Bmatrix}\cos(n\varphi) + \begin{Bmatrix}D_{nq2}^E\\ D_{nq2}^H\end{Bmatrix}\sin(n\varphi)\right]\exp(qz)\right\}.$$

Finally, for the field strengths $\boldsymbol{E}_3$, $\boldsymbol{H}_3$ in a half-space 3 ($z < -h$), we have

$$\boldsymbol{E}_3 = -\nabla\phi_3^E,\ \boldsymbol{H}_3 = -\nabla\phi_3^H,\ \begin{Bmatrix}\phi_3^E\\ \phi_3^H\end{Bmatrix} = \sum_{n=0}^{1}\int_0^\infty \mathrm{d}q q J_n(q\rho)\times$$

$$\times\left[\begin{Bmatrix} C^{E}_{nq3} \\ C^{H}_{nq3} \end{Bmatrix}\cos(n\varphi) + \begin{Bmatrix} D^{E}_{nq3} \\ D^{H}_{nq3} \end{Bmatrix}\sin(n\varphi)\right]\exp(qz). \qquad (6)$$

To find the coefficients in (4)–(6) one should make use of the conditions of the continuity of the potentials on the surfaces of the interface separating the media and of the continuity of the normal component of the induction. To determine the inductions in the layer, we substitute Maxwell's equations into (1) and obtain

$$\boldsymbol{D}_2 = \frac{\varepsilon_2(\boldsymbol{E}_2 + \mathrm{i}\chi_2\mu_2\boldsymbol{H}_2)}{1-\chi_2^2\varepsilon_2\mu_2},\ \boldsymbol{B}_2 = \frac{\mu_2(\boldsymbol{H}_2 - \mathrm{i}\chi_2\varepsilon_2\boldsymbol{E}_2)}{1-\chi_2^2\varepsilon_2\mu_2}. \qquad (7)$$

From (7) it follows that inside the chiral layer the electric and magnetic fields are related. In the case of a non-chiral medium ($\chi_2 = 0$) one can derive from (7) regular expressions for the induction.

Relations (7) allow us to write the boundary conditions. After substituting the potentials of Eqns (3)–(6) into them, we find the required coefficients. Because the expressions for the coefficients are very cumbersome, they are given in the Appendix.

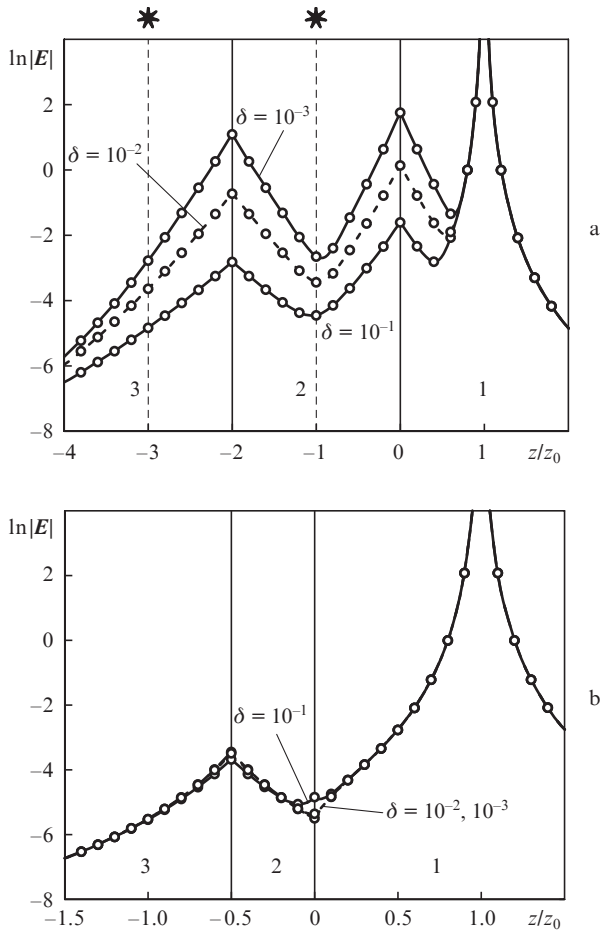


**Figure 3.** Logarithm of the modulus of the total electric field [see Eqns (2), (4)–(6)] ($\boldsymbol{E}$ – in rel. units) as a function of $z/z_0$ ($x = y = 0$) for a thin chiral DNG layer with $\varepsilon_2 = \mu_2 = -2 + \mathrm{i}\delta$ and $\chi_2 = +1/2$ at different $\delta$ in the case of a dipole with $\boldsymbol{d}_0 \parallel x$ and $\boldsymbol{m}_0 = 0$. Points show the resulting solutions with the retardation [12] taken into account at $k_0 z_0 = 0.1$. The layer thickness is $h =$ (a) $2z_0$ and (b) $z_0/2$. Here and in Figs 4–6, numbers 1, 2, 3 denote the media in accordance with Fig.2. Asterisks indicate the positions of the foci in accordance with Fig. 1.

In our previous work [13] we showed that the following conditions are good for focusing dipole radiation by a negative index chiral metamaterial layer whose thickness is compared with the wavelength: $z_0 < h$, $\varepsilon_2 = \mu_2 = -2 + \mathrm{i}\delta$ ($\delta \to 0$) and $\chi_2 = \pm 1/2$. When these conditions are met, predominantly right- or left-hand polarised waves (depending on the sign of $\chi_2$), for which the wavenumber is close to $-k_0$, propagate in the layer. We will consider a thin chiral DNG layer under the same conditions.

Figure 3 shows the dependences of the logarithm of the modulus of the electric field [see Eqn (2), (4)–(6)] on $z/z_0$ ($x = y = 0$) for a thin layer of a negative index chiral metamaterial. It is clearly seen (Fig. 3a) that when $z_0 < h$, the highest (in modulus) values of the induced field are localised on the surfaces of the interfaces separating the media rather than at points of intersection of the rays (see Fig. 1), and focusing in its strict sense does not arise at all . A similar result is obtained from the total (taking into account the retardation) solution to the problem of the dipole in the vicinity of the chiral DNG layer [13]. It is also seen that when the losses in the layer tend to zero ($\delta \to 0$), the induced field increases indefinitely. In fact, plasmon waves of unlimited amplitude are excited on the layer surfaces.

When $z_0 > h$, the maximum of the modulus of the induced electric field is localised on the layer surface that is farthest from the source, i.e., between media 2 and 3 (Fig. 3b). However, in this case, when the losses tend to zero in the layer, the modulus of the field experiences no significant changes. Note that in this case focusing is not expected.

## 3. A point source near a lossless chiral layer (quasi-static approximation)

As can be seen from the previous section, in the case of $z_0 < h$ and losses tending to zero in the chiral DNG layer, the solution tends to infinity in the entire space, i.e., does not exist. This is due to the resonant excitation of surface plasmon waves.

However, this raises the question: Is there a sensible solution in this region of the parameters?

In the case of a lossless DNG layer ($\delta = 0$) the formal expressions for the potentials obtained from (3)–(6) have the form (here and what follows the 'upper' sign corresponds to $\chi_2 = +1/2$, and the 'lower' sign – to $\chi_2 = -1/2$)

$$-\phi_1^E = \pm\mathrm{i}\phi_1^H = -\frac{1}{2}(d_{0z} \mp \mathrm{i}m_{0z})\int_0^\infty \mathrm{d}qqJ_0(q\rho)\exp[-q(z+z_0)]$$

$$+\frac{1}{2}[(d_{0x} \mp \mathrm{i}m_{0x})\cos\varphi + (d_{0y} \mp \mathrm{i}m_{0y})\sin\varphi] \qquad (8)$$

$$\times\int_0^\infty \mathrm{d}qqJ_1(q\rho)\exp[-q(z+z_0)] \quad (z > 0),$$

$$\phi_2^E = \pm\mathrm{i}\phi_2^H = -\frac{1}{2}(d_{0z} \pm \mathrm{i}m_{0z})\int_0^\infty \mathrm{d}qqJ_0(q\rho)\exp[-q(z+z_0)]$$

$$+\frac{1}{2}[(d_{0x} \pm \mathrm{i}m_{0x})\cos\varphi + (d_{0y} \pm \mathrm{i}m_{0y})\sin\varphi] \qquad (9)$$

$$\times\int_0^\infty \mathrm{d}qqJ_1(q\rho)\exp[-q(z+z_0)] \quad (-h < z < 0),$$

$$\phi_3^E = \pm i\phi_3^H = -\frac{1}{2}(d_{0z} \pm im_{0z})\int_0^\infty dqqJ_0(q\rho)\exp[q(z - z_0 + 2h)]$$

$$+ \frac{1}{2}[(d_{0x} \pm im_{0x})\cos\varphi + (d_{0y} \pm im_{0y})\sin\varphi] \qquad (10)$$

$$\times \int_0^\infty dqqJ_1(q\rho)\exp[q(z - z_0 + 2h)] \quad (z < -h).$$

Integrals in (8)–(10) converge only at certain values of $z$. If $z_0 < h$, solution (9) in the region $z_0 < |z| < h$ and solution (10) in the region $h < |z| < 2h - z_0$ increase indefinitely (plasmon waves). At the same time, when $z_0 > h$, solutions (9) and (10) exist for all $z$ and surface plasmon waves are not excited.

For a bounded solution to be obtained in a lossless chiral metamaterial layer ($\delta = 0$) in the case of $z_0 < h$, we use the method of analytic continuation [6–8]. To this end, we integrate formal solutions (8)–(10) in the regions of convergence and then analytically continue the obtained expressions to the region $z_0 < h$, where the integrals diverge. As a result, the expressions

$$-\phi_1^E = \pm i\phi_1^H = -\frac{1}{2}(\tilde{\boldsymbol{d}}_0 \pm i\tilde{\boldsymbol{m}}_0)\nabla\frac{1}{|\boldsymbol{r} - \boldsymbol{r}_C|} \quad (z > 0),$$

$$\phi_2^E = \pm i\phi_2^H = -\frac{1}{2}(\tilde{\boldsymbol{d}}_0 \pm i\tilde{\boldsymbol{m}}_0)\nabla\frac{1}{|\boldsymbol{r} - \boldsymbol{r}_C|} \quad (-h < z < 0), \qquad (11)$$

$$\phi_3^E = \pm i\phi_3^H = -\frac{1}{2}(\boldsymbol{d}_0 \pm i\boldsymbol{m}_0)\nabla\frac{1}{|\boldsymbol{r} - \boldsymbol{r}_B|} \quad (z < -h)$$

will hold for the potential in the entire space, where $\boldsymbol{r}_C = -z_0\boldsymbol{e}_z$; $\boldsymbol{r}_B = -(2h - z_0)\boldsymbol{e}_z$; $\tilde{\boldsymbol{d}}_0 = \boldsymbol{d}_0 - 2d_{0z}\boldsymbol{e}_z$; $\tilde{\boldsymbol{m}}_0 = \boldsymbol{m}_0 - 2m_{0z}\boldsymbol{e}_z$; and $\boldsymbol{e}_z$ is the unit vector along the $z$ axis. From (11) it follows that for the bounded solution to exist at $z_0 < h$ for a source with electric and magnetic dipole moments $\boldsymbol{d}_A = \boldsymbol{d}_0$ and $\boldsymbol{m}_A = \boldsymbol{m}_0$, located at point A with coordinates $\boldsymbol{r}_A = \boldsymbol{r}_0$ near a lossless metamaterial layer, a source with the electric and magnetic dipole moments $\boldsymbol{d}_C = (\tilde{\boldsymbol{d}}_0 \pm i\tilde{\boldsymbol{m}}_0)/2$ and $\boldsymbol{m}_C = (\tilde{\boldsymbol{m}}_0 \mp i\tilde{\boldsymbol{d}}_0)/2$ should be placed at point C with coordinates $\boldsymbol{r}_C$ and a source with electric and magnetic dipole moments $\boldsymbol{d}_B = (\boldsymbol{d}_0 \pm i\boldsymbol{m}_0)/2$ and $\boldsymbol{m}_B = (\boldsymbol{m}_0 \mp i\boldsymbol{d}_0)/2$ should be placed behind the layer at point B with coordinates $\boldsymbol{r}_B$. Note that points A, B and C correspond to points of intersection of the rays in the geometric model of a perfect lens (see Fig. 1). The found expressions (11) satisfy the boundary conditions both at $z_0 > h$ and at $z_0 < h$.

Importantly, solution (11) does not have singularities at $z_0 > h$, while at $z_0 < h$ in the layer and behind it, solution (11) already contains real singularities. It is also important that solution (11) at $z_0 < h$ with three singularities is stable and addition of small losses in the system has no significant effect. From a physical point of view, the system of sources (11) has such symmetry that plasmon waves on the layer surfaces are not excited!

The electric field for the obtained solution (11) is shown in Fig. 4. One can see from Figs 3 and 4 that at $z_0 > h$ (Fig. 4b) solution (11) is virtually identical to the conventional general solution (Fig. 3b). However, when $z_0 < h$, the solutions differ significantly (cf. Figs 3a and 4a). The conventional solution in the limit $\delta = 0$ has singularities at the layer boundaries (running plasmons of unlimited amplitude), while solution (11) has singularities only at points corresponding to the intersection of rays in Fig. 1 (asterisks in Fig. 4a). In fact, in the limit $\delta = 0$ uniqueness of the solution is lost (bifurcation).

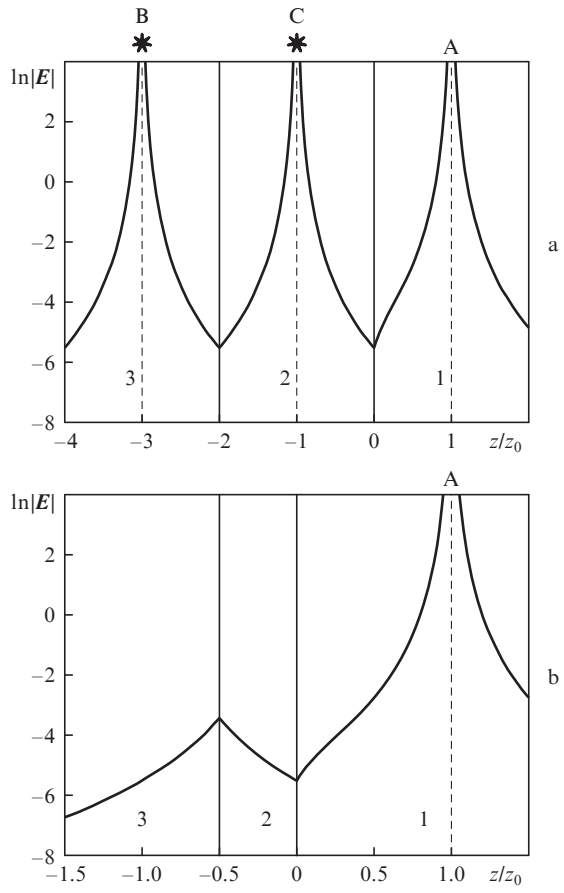


**Figure 4.** Logarithm of the modulus of the total electric field [see Eqns (2) and (11)] ($\boldsymbol{E}$ – in rel. units) as a function of $z/z_0$ ($x = y = 0$) for a thin lossless chiral DNG layer with $\varepsilon_2 = \mu_2 = -2$ and $\chi_2 = +1/2$ in the case of a dipole with $\boldsymbol{d}_0 \parallel x$ and $\boldsymbol{m}_0 = 0$. The layer thickness is $h =$ (a) $2z_0$ and (b) $z_0/2$. Points A, B and C correspond to the positions of the primary (A) and additional (B and C) radiation sources. Asterisks indicate the positions of the foci in accordance with Fig. 1.

Figure 5 shows the electric potentials for low-loss and lossless systems when the source is located at different distances from the chiral DNG layer.

In a conventional Veselago perfect lens the reflected field is absent. As follows from (11), to suppress the field reflected from the chiral DNG layer we should set $\boldsymbol{d}_0 = \pm i\boldsymbol{m}_0$. In this particular case, we obtain

$$\boldsymbol{d}_A = \boldsymbol{d}_0,\ \boldsymbol{m}_A = \mp i\boldsymbol{d}_A,$$

$$\boldsymbol{d}_C = \tilde{\boldsymbol{d}}_0,\ \boldsymbol{m}_C = \mp i\boldsymbol{d}_C, \qquad (12)$$

$$\boldsymbol{d}_B = \boldsymbol{d}_0,\ \boldsymbol{m}_B = \mp i\boldsymbol{d}_B.$$

If we set $\boldsymbol{d}_0 = \mp i\boldsymbol{m}_0$ in (11), the fields in media 2 and 3 are equal to zero. Then, the thin lossless chiral DNG layer in question will be a 'mirror' for the radiation source. This interesting effect will be discussed in a separate paper in more detail.

Thus, in this section, using the method of analytic continuation we have found the solution, the position of the singularities in which coincides with the points of intersection of rays in Fig. 1. To clarify the physical meaning of the solution obtained it is necessary to consider the problem in view of the retardation, which will be done in the next section.

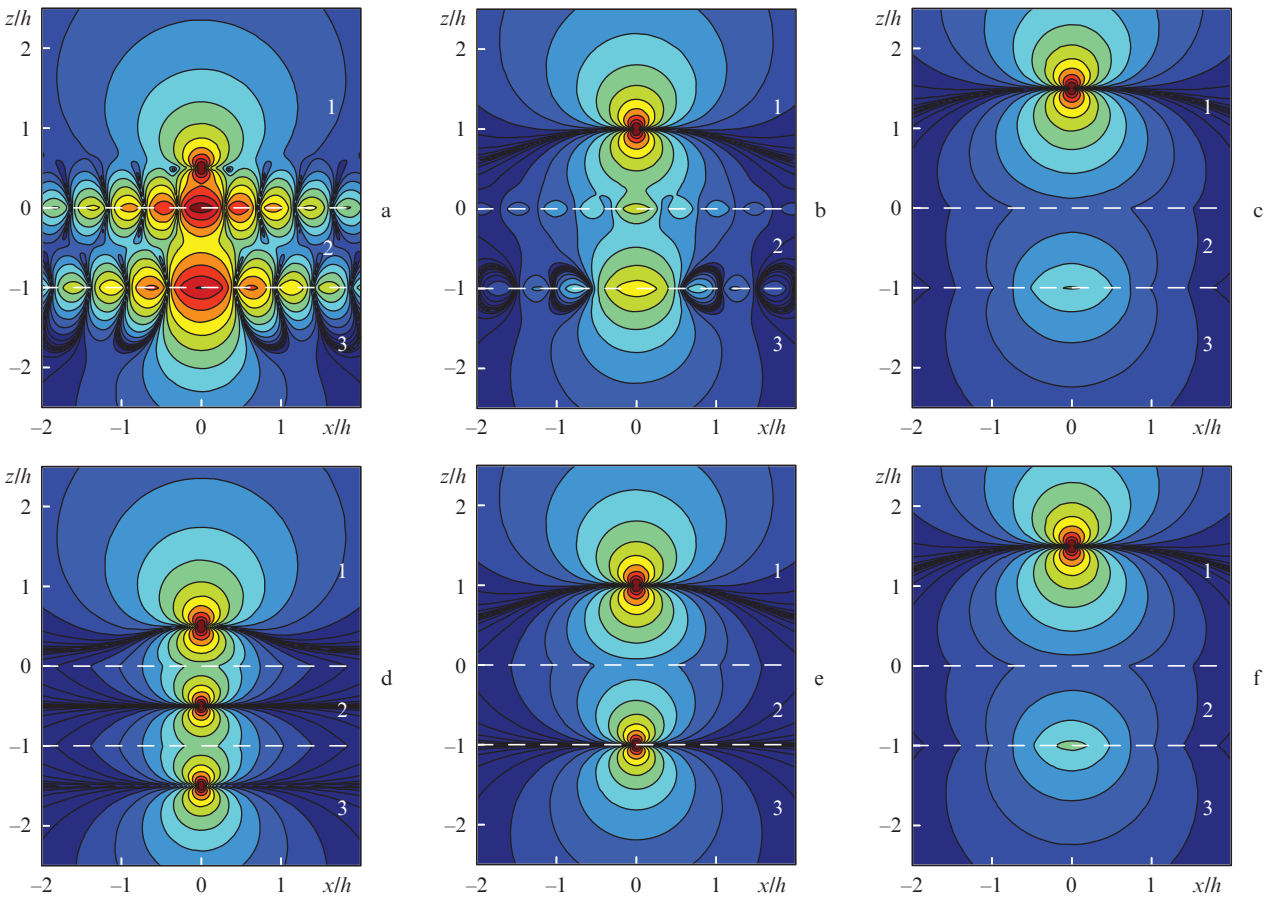


**Figure 5.** Logarithm of the modulus of the total electric potential ($\phi^E$ – in rel. units) in the plane $y = 0$ for a thin chiral DNG layer with $\varepsilon_2 = \mu_2 = -2 + i\delta$ and $\chi_2 = +1/2$ in the case of a dipole with $\boldsymbol{d}_0 \parallel z$ and $\boldsymbol{m}_0 = 0$ for low-loss [$\delta = 10^{-2}$, (a–c)] and lossless [$\delta = 0$, (d–f)] layers when the source is located at a distance $z_0$ = (a, d) $h/2$, (b, e) $h$ and (c, f) $3h/2$. The bright areas correspond to large values of $|\phi^E|$, and dark – to small.

## 4. Account for the retardation effects

A surprising feature of the quasi-static solution found in Section 3 is that it allows simple but accurate generalisation to the case of retardation. To this end, it suffices to replace the electrostatic Green functions for the solution outside the layer by the retarded Green functions ($J$ = A, B):

$$\frac{1}{|\boldsymbol{r}-\boldsymbol{r}_J|} \to \frac{\exp(ik_0|\boldsymbol{r}-\boldsymbol{r}_J|)}{|\boldsymbol{r}-\boldsymbol{r}_J|}. \tag{13}$$

For the solution inside layer it is necessary to make a similar transformation, but in this case we must take into account that, depending on the sign of $\chi_2 = \pm 1/2$ ($\varepsilon_2 = \mu_2 = -2$), either left-hand polarised (L) or right-hand polarised (R) waves can propagate in a lossless chiral DNG layer [13]:

$$\begin{gathered}\frac{1}{|\boldsymbol{r}-\boldsymbol{r}_C|} \to \frac{\exp(-ik_L|\boldsymbol{r}-\boldsymbol{r}_C|)}{|\boldsymbol{r}-\boldsymbol{r}_C|},\\ k_L = \frac{k_0\sqrt{\varepsilon_2\mu_2}}{1-\chi_2\sqrt{\varepsilon_2\mu_2}} \to -k_0 \ (\chi_2 = +1/2),\\ \frac{1}{|\boldsymbol{r}-\boldsymbol{r}_C|} \to \frac{\exp(-ik_R|\boldsymbol{r}-\boldsymbol{r}_C|)}{|\boldsymbol{r}-\boldsymbol{r}_C|},\\ k_R = \frac{k_0\sqrt{\varepsilon_2\mu_2}}{1+\chi_2\sqrt{\varepsilon_2\mu_2}} \to -k_0 \ (\chi_2 = -1/2).\end{gathered} \tag{14}$$

As a result, explicit expressions for the electric and magnetic field strengths in the case of dipoles (12), when there is no reflected field, take the form

$$\begin{gathered}\boldsymbol{E}_1 = [(\boldsymbol{d}_A\nabla)\nabla + k_0^2\boldsymbol{d}_A]\frac{\exp(ik_0|\boldsymbol{r}-\boldsymbol{r}_A|)}{|\boldsymbol{r}-\boldsymbol{r}_A|}\\ + ik_0\,\mathrm{rot}\left[\frac{\boldsymbol{m}_A\exp(ik_0|\boldsymbol{r}-\boldsymbol{r}_A|)}{|\boldsymbol{r}-\boldsymbol{r}_A|}\right],\ \boldsymbol{H}_1 = -\frac{i}{k_0}\mathrm{rot}\boldsymbol{E}_1 \ (z > 0),\\ \boldsymbol{E}_2 = [(\boldsymbol{d}_C\nabla)\nabla + k_0^2\boldsymbol{d}_C]\frac{\exp(ik_0|\boldsymbol{r}-\boldsymbol{r}_C|)}{|\boldsymbol{r}-\boldsymbol{r}_C|}\\ - ik_0\,\mathrm{rot}\left[\frac{\boldsymbol{m}_C\exp(ik_0|\boldsymbol{r}-\boldsymbol{r}_C|)}{|\boldsymbol{r}-\boldsymbol{r}_C|}\right],\ \boldsymbol{H}_2 = \frac{i}{k_0}\mathrm{rot}\boldsymbol{E}_2 \ (-h < z < 0),\\ \boldsymbol{E}_3 = [(\boldsymbol{d}_B\nabla)\nabla + k_0^2\boldsymbol{d}_B]\frac{\exp(ik_0|\boldsymbol{r}-\boldsymbol{r}_B|)}{|\boldsymbol{r}-\boldsymbol{r}_B|}\\ + ik_0\,\mathrm{rot}\left[\frac{\boldsymbol{m}_B\exp(ik_0|\boldsymbol{r}-\boldsymbol{r}_B|)}{|\boldsymbol{r}-\boldsymbol{r}_B|}\right],\ \boldsymbol{H}_3 = -\frac{i}{k_0}\mathrm{rot}\boldsymbol{E}_3 \ (z < -h).\end{gathered} \tag{15}$$

As follows from (15), radiation sources (12) produce circularly polarised waves, and the chiral layer has an effective

refractive index equal to –1. Note that expressions (15) satisfy the boundary conditions for all $z_0$.

Figure 6 shows the energy flow (Poynting vector) $\boldsymbol{S} = [c/(8\pi)]\mathrm{Re}[\boldsymbol{EH}^*]$ for solution (15) in the plane $y = 0$. One can see that the flows of energy for a primary source located in the $z_0 < h$ region are directed to an additional source inside the layer (sink) rather than outside the layer, as it would occur in a perfect lens (see Figs 1 and 6a). When moving the primary source to the region $z_0 > h$, singularities in the solution for the fields in the layer and behind the layer do not arise, and the energy flow in this case is directed behind the layer (Fig.6b).

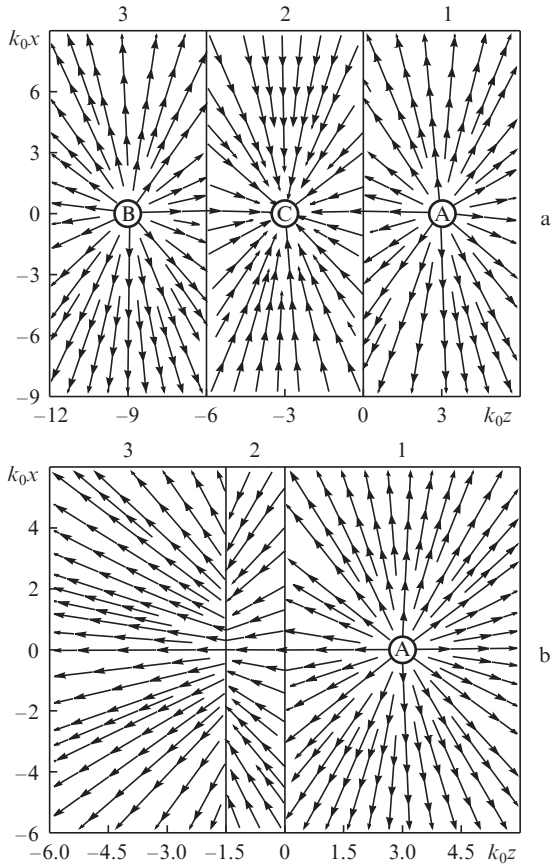


**Figure 6.** Energy flow in the plane $y = 0$ for a lossless chiral DNG layer with $\varepsilon_2 = \mu_2 = -2$ and $\chi_2 = +1/2$ [see Eqn (15)]. The layer thickness is $h =$ (a) $2z_0$ and (b) $z_0/2$. The source with $\boldsymbol{d}_\mathrm{A} \parallel y$ is located at point $k_0z_0 = 3$. Points A, B and C correspond to the positions of the primary (A) and additional (B and C) radiation sources.

A similar behaviour of the Poynting vector also occurs in considering the problem of emission of the main and additional electric dipoles near the layer with a refractive index –1, studied in papers [6–8]. The resulting solution there may be a basis for creation of unique devices – perfect coherent nanoabsorbers [10, 11] – or for resonant excitation of atoms with high probability. Solution (15) found in the present study is more complex, i.e., requires the presence of chiral radiation sources with electric and magnetic dipole moments equal in absolute value. However, the solution presented here makes it possible to produce a perfect coherent absorber of circularly polarised waves and elements of quantum computers.

## 5. Conclusions

Thus, using the quasi-static approximation and a complete system of Maxwell's equations we have obtained and investigated analytical expressions for the electromagnetic fields of a chiral dipole (electric and magnetic) source located near a thin layer of a negative index chiral material.

It is shown that for a chiral dipole source located at a distance greater than the thickness of the layer, the solution can be represented in the form of two additional (imaginary) chiral point sources. When the source is located at a distance from the source layer that is smaller than its thickness, imaginary sources must be replaced with real ones to obtain the bounded solution. The resulting solution is generalised to the case taking into account the retardation effects for an arbitrary thick layer as compared with wavelength.

Note that the solution was found for special values of permittivity and permeability and chirality parameter and is not unique. The study of the whole class of new solutions for the chiral metamaterial layer will be described in a separate publication.

The results obtained in the present study can be used to calculate the scattering of electromagnetic radiation of a dipole source by a layer of thin chiral metamaterial, to interpret the experimental results and to develop new focusing devices on the basis of circularly polarised waves. The main feature of such devices will be either an absorbing nanoparticle, or even a single atom located at a point of the energy sink, predicted by our solution (point C in Fig. 6).

***Acknowledgements.*** The authors express their gratitude to the Belarusian Republican Foundation for Fundamental Research (Grant No. F12R-006), Russian Foundation for Basic Research (Grant No. 14-02-00290), Skolkovo Foundation and Russian Quantum Centre for the financial support of this work.

## Appendix. Explicit form of the coefficients in expressions (4)–(6)

The coefficients appearing in (4)–(6) can be represented in the form:

$$\begin{Bmatrix} A^E_{nq1} \\ B^E_{nq1} \end{Bmatrix} = -\frac{1}{2}\begin{Bmatrix} A^E_{nq} \\ B^E_{nq} \end{Bmatrix}\sinh(2qh)\{2\mu_2(\varepsilon_2^2 - 1 + \chi_2^2\varepsilon_2\mu_2)$$

$$+ [\varepsilon_2^2 - \mu_2^2 + \varepsilon_2^2\mu_2^2 - (1 - \chi_2^2\varepsilon_2\mu_2)^2]\tanh(2qh)\}\frac{1}{\Delta}$$

$$- \mathrm{i}\chi_2\varepsilon_2\mu_2\begin{Bmatrix} A^H_{nq} \\ B^H_{nq} \end{Bmatrix}\sinh(2qh)$$

$$\times[\varepsilon_2\mu_2 + 1 - \chi_2^2\varepsilon_2\mu_2 + (\varepsilon_2 + \mu_2)\tanh(qh)]\frac{1}{\Delta}, \qquad \text{(A1)}$$

$$\begin{Bmatrix} A^E_{nq2} \\ B^E_{nq2} \end{Bmatrix}\exp(qh) = \begin{Bmatrix} A^E_{nq} \\ B^E_{nq} \end{Bmatrix}\cosh(qh)\{2\mu_2(\varepsilon_2 - 1)(1 - \chi_2^2\varepsilon_2\mu_2)$$

$$+ [(\varepsilon_2 - 1 + \chi_2^2\varepsilon_2\mu_2)(1 - \chi_2^2\varepsilon_2\mu_2) + \mu_2^2(\varepsilon_2 - 1 - \chi_2^2\varepsilon_2^2)]\tanh(qh)\}\frac{1}{\Delta}$$

$$+ \mathrm{i}\chi_2\varepsilon_2\mu_2\begin{Bmatrix} A^H_{nq} \\ B^H_{nq} \end{Bmatrix}\cosh(qh)[2(1 - \chi_2^2\varepsilon_2\mu_2) +$$

$$+(\varepsilon_2+\mu_2-\varepsilon_2\mu_2+1-\chi_2^2\varepsilon_2\mu_2)\tanh(qh)]\frac{1}{\Delta}, \quad \text{(A2)}$$

$$\begin{Bmatrix} C^E_{nq2} \\ D^E_{nq2} \end{Bmatrix}\exp(-qh) = \begin{Bmatrix} A^E_{nq} \\ B^E_{nq} \end{Bmatrix}\cosh(qh)\{2\mu_2(\varepsilon_2+1)(1-\chi_2^2\varepsilon_2\mu_2)$$

$$+[(\varepsilon_2+1-\chi_2^2\varepsilon_2\mu_2)(1-\chi_2^2\varepsilon_2\mu_2)+\mu_2^2(\varepsilon_2+1+\chi_2^2\varepsilon_2^2)]\tanh(qh)\}\frac{1}{\Delta}$$

$$-i\chi_2\varepsilon_2\mu_2\begin{Bmatrix} A^H_{nq} \\ B^H_{nq} \end{Bmatrix}\cosh(qh)[2(1-\chi_2^2\varepsilon_2\mu_2)$$

$$+(\varepsilon_2+\mu_2+\varepsilon_2\mu_2-1+\chi_2^2\varepsilon_2\mu_2)\tanh(qh)]\frac{1}{\Delta}, \quad \text{(A3)}$$

$$\begin{Bmatrix} C^E_{nq3} \\ D^E_{nq3} \end{Bmatrix}\exp(-qh) = 2\varepsilon_2\begin{Bmatrix} A^E_{nq} \\ B^E_{nq} \end{Bmatrix}\cosh(qh)$$

$$\times[2\mu_2(1-\chi_2^2\varepsilon_2\mu_2)+(\mu_2^2+1-\chi_2^2\varepsilon_2\mu_2)\tanh(qh)]\frac{1}{\Delta}-$$

$$-2i\chi_2\varepsilon_2\mu_2\begin{Bmatrix} A^H_{nq} \\ B^H_{nq} \end{Bmatrix}\sinh(qh)(\varepsilon_2\mu_2-1+\chi_2^2\varepsilon_2\mu_2)\frac{1}{\Delta}, \quad \text{(A4)}$$

where

$$\Delta = \cosh^2(qh)\{4\varepsilon_2\mu_2(1-\chi_2^2\varepsilon_2\mu_2)$$

$$+2(\varepsilon_2+\mu_2)(\varepsilon_2\mu_2+1-\chi_2^2\varepsilon_2\mu_2)\tanh(qh)$$

$$+[(\varepsilon_2+\mu_2)^2+\varepsilon_2^2\mu_2^2$$

$$-(2\varepsilon_2\mu_2-1+\chi_2^2\varepsilon_2\mu_2)(1-\chi_2^2\varepsilon_2\mu_2)]\tanh^2(qh)\}; \quad \text{(A5)}$$

$$A^E_{nq}=(-\delta_{n0}d_{0z}+\delta_{n1}d_{0x})\exp(-qz_0);\ B^E_{nq}=\delta_{n1}d_{0y}\exp(-qz_0);$$

$$A^H_{nq}=(-\delta_{n0}m_{0z}+\delta_{n1}m_{0x})\exp(-qz_0);\ B^H_{nq}=\delta_{n1}m_{0y}\exp(-qz_0); \quad \text{(A6)}$$

and $\delta_{np}$ is the Kronecker delta equal to 1 at $n = p$ and to zero in other cases.

The expressions for the other coefficients in (4)–(6) can be obtained from (A1)–(A4) by using the permutation of the superscripts $E \leftrightarrow H$, permittivity and permeability $\varepsilon_2 \leftrightarrow \mu_2$ and the replacement $\chi_2 \to -\chi_2$.

## References


1. Sommerfeld A. *Ann. Phys.*, **28**, 665 (1909).
2. Banos A. *Dipole Radiation in the Presence of a Conducting Half-Space* (Oxford: Pergamon Press, 1966).
3. Veselago V.G. *Usp. Fiz. Nauk*, **92**, 517 (1967) [*Sov. Phys. Usp.*, **10**, 509 (1968)].
4. Pendry J.B. *Phys. Rev. Lett.*, **85**, 3966 (2000).
5. Merlin R. *Appl. Phys. Lett.*, **84**, 1290 (2004).
6. Klimov V.V. *Pis'ma Zh. Teor. Eksp. Fiz.*, **89** (5), 270 (2009).
7. Klimov V.V. http://demonstrations.wolfram.com/EnergyFlowInANegativeIndexMaterial/.
8. Klimov V., Baudon J., Ducloy M. *Europhys. Lett.*, **94**, 20006 (2011).
9. Bergman D. *J. Phys. Rev. A*, **89**, 015801 (2014).
10. Klimov V., Sun S., Guo G.-Y. *Opt. Express*, **20**, 13071 (2012).
11. Guo G.-Y., Klimov V., Sun S., Zheng W.-J. *Opt. Express*, **21**, 11338 (2013).
12. Pendry J.B. *Science*, **306**, 1353 (2004).
13. Guzatov D.V., Klimov V.V. *Kvantovaya Elektron.*, **44**, 873 (2014) [*Quantum Electron.*, **44**, 873 (2014)].
14. Drude P. *Lehrbuch der Optik* (Leipzig: Verlag von S.Hirzel, 1906).
15. Born M. *Optika: uchebnik elektromagnitnoi teorii sveta* (Optics: A Textbook on the Electromagnetic Theory of Light) (Kharkov–Kiev: GNTI Ukrainy, 1937).
16. Bokut B.V., Serdyukov A.N., Fedorov F.I. *Kristallographiya*, **15**, 1002 (1970) [*Sov. Phys. Crystallogr.*, **15**, 871 (1971)].
17. Morse P.M., Feshbach H. *Methods of Theoretical Physics* (New York: McGraw Hill, 1953; Moscow: IL, 1960) Vol. 2.
18. Abramowitz M., Stegun I. *Handbook of Mathematical Functiuons* (New York: Dover, 1965; Moscow: Nauka, 1979).